MEASUREMENTS AND SIMULATIONS OF LONGITUDINAL RELAXATION OSCILLATIONS INDUCED BY HOMs*

C.Limborg, J.Sebek, SSRL/SLAC, Stanford, CA

Abstract

Although the linear theory of stable and unstable synchrotron oscillations has long been understood, there is no such satisfactory description of the large amplitude highly non-linear synchrotron motion. With an appropriate tuning of RF cavity impedance, large amplitude, low frequency, self-sustained relaxation oscillations of this synchrotron motion can be observed. This paper presents experimental data and computer simulations that give insights into the details of the mechanism involved.

1 INTRODUCTION

The voltage induced by the beam on the cavity impedance, at the upper synchrotron sideband of the revolution harmonics has a destabilizing effect on the beam. The instability commonly known as the coupled bunch instability occurs when this force exceeds the net damping force. On the SPEAR electron storage ring, such an instability can be produced from a multi-traversal effect acting on a single bunch. Linear theory predicts that above instability threshold the amplitude of the bunch synchrotron oscillation would grow to infinity. However, it has been long observed [1] [2] that the amplitude of oscillation can also saturate. In particular, at the onset of instability, there exists a regime in which the bunch performs relaxation oscillations. Extensive measurements were performed to give the details which constitute the basis of the theoretical model explaining the physics of the mechanism [3].

2 EXPERIMENTAL RESULTS

2.1 Motivations

While characterizing the RF cavities in order to improve the stability of SPEAR and focusing our attention on the growth of the HOM induced instabilities, a regular modulation about the saturation level was observed (figure (1a)) [4]. Its period was always longer than a radiation damping time. This modulation is often small, but certain machine parameters can make it very large, regular, and quite striking (figure (1b)). The possibility of adjusting the HOM frequency, by positioning a moveable RF cavity tuner in the passive RF cavity, made such observations very repeatable and convenient to study on the SPEAR ring.

2.2 Experimental parameters

The experimental parameters are presented in table 1. The

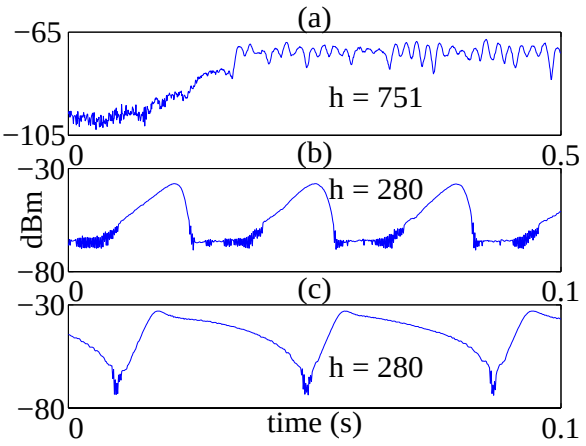

Figure 1: Output from the cavity signal at h$f_0 + f_s$. Note the different growth and damping rates in (b) and (c).

Energy	$\mathbf{U}_0$	$\mathbf{V}_{RF}$	τ_{damp}	$\mathbf{R}_S$
2.3 GeV	193 keV	1.68 MV	10 ms	10 MΩ

Table 1: Machine parameters

resonance studied is the fundamental resonance, $f_{HOM} = f_{RF}$. The large variety of time scales involved in the relaxation mechanism is presented in table 2.

2.3 Description of measurements

Since the effect of interest depends on the HOM strength, the largest available impedance was chosen for the study. SPEAR has two RF cavities, but only one is powered for normal operation. Therefore, the largest available impedance is the fundamental mode of the idle RF cavity; this mode was chosen for our study. The strength of this impedance means that the HOM produces a strong long-range wakefield at currents for which the short-range effects of the wakefield are not very important. (In this paper, liberty has been taken with the term HOM, since here

	Frequency	Period	N_{turns}
$f_{sawtooth}$	< 100 Hz	> 10 ms	> 12800
f_{so}	28.4 kHz	35 μs	45
α_R	56 kHz	17.8 μs	23
f_o	1.28 MHz	0.78 μs	1
$f_{RF} = f_{HOM}$	358.5 MHz	2.8 ns	$1/280$
$(1/\sigma_\tau)$	10 GHz	100 ps	$1/7840$

Table 2: System time scales

* Work supported by the Department of Energy, contract DE-AC03-76SF00515.

it also refers to the fundamental mode in the idle cavity.)

Spectrum analyzer Data were first taken on an RF spectrum analyzer from an RF signal coming from an RF cavity probe (figure 1). The spectrum analyzer was used as a narrowband receiver, in zero-span mode, tuned on the upper synchrotron sideband of the fundamental RF harmonic. Its resolution bandwidth, 10 kHz, allowed reasonable rejection of the RF harmonic while preserving the ability to see fast dynamic changes in the amplitude of the sideband over the variation of the synchrotron frequency during the relaxation oscillation.

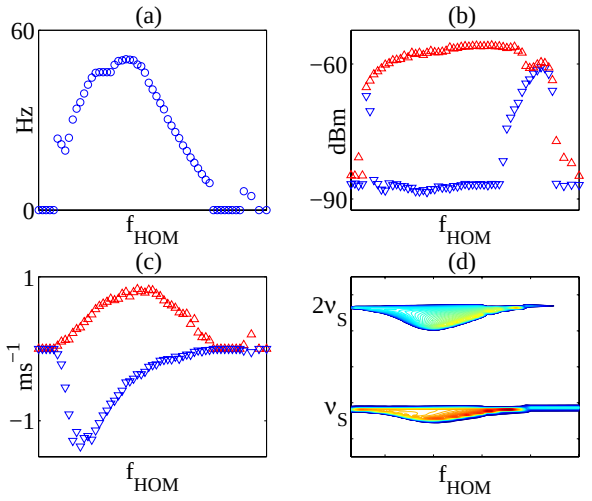

Figure 2: Relaxation oscillation parameters vs f_{HOM}: (a) relaxation oscillation frequency, (b) maximum ($\triangle$) and minimum ($\triangledown$) power of oscillation, (c) growth times ($\triangle$) and damping times ($\triangledown$), (d) ν_s, showing $\sim 15\%$ deviation over the range of f_{HOM}.

The evolution of crucial parameters of the relaxation oscillation as a function of the resonator frequency is summarized in figure 2. From the amplitude information, (2b), one sees that the amplitude of oscillation is large along most of the resonance. The growth rate, as a function of frequency, is symmetric with respect to the center frequency, (2c). It correlates with the resistive part of the resonator impedance. The damping rate is not nearly as symmetric (2c). It is very small over the second half of the resonance curve (2b). Because of this asymmetry, the frequency of this relaxation oscillation (2a) as a function of the HOM frequency is also asymmetric.

Digital spectrum analyzer The variation and/or spread of the synchrotron tune during these oscillations was also measured. This data was obtained by observing the demodulation of a signal coming from a ring pickup on a digital spectrum analyzer. Since the analyzer averaged over many relaxation periods, this measurement could not resolve the difference between a tune variation and a spread over the oscillation. The frequency deviation showed a decrease of 15% from the nominal synchrotron frequency, corresponding to the shift for large amplitude pendulum oscillations (figure (2d)).

Streak camera The spectrum analyzer data only gives information about the dipole moment of the beam. With a streak camera, details about the internal structure of the beam could be observed. Data were taken both at a slow scan rate, i.e. slow enough to see the entire relaxation oscillation cycle, and at a fast rate, at which one could see the single bunch every third revolution period.

On the slow scan range, the entire relaxation oscillation cycle was captured. While growing, the envelope visible in the slow scan shows the bunch to be concentrated near the extremes of the oscillation. But its charge density decreases with time (figure 3a). The maximum amplitude of oscillation reached is about $\pi/2$ radians. In the damping phase, this macroparticle still exists and damps, but it has a much reduced intensity compared to its initial value. At the end of this phase, particles have accumulated around the center. In the particular case of f_{HOM} slightly above $pf_0 + f_{so}$, when the damping is very slow, a second accumulation point clearly forms near the origin (figure 3b). The charge at this point grows in both amplitude and intensity as the original macroparticle continues its decay. The second accumulation point, when seen, is phase-locked to the initial macroparticle, but approximately π out of phase with it (figure (3c)(3d)).

As a summary, the oscillation starts when one center grows exponentially, then saturates and loses particles, and finally begins to damp. These lost particles accumulate at a second center which grows, accumulating more particles, as the first center migrates to the origin while still losing its charge. The two centers have now exchanged roles in this oscillation, giving the system its bistable character.

3 SIMULATIONS

3.1 Simulation program

The multiparticle simulation code gives the evolution of the phase space distribution of a single bunch, turn after turn, in the presence of a perturbing long range wakefield. As the streak camera images showed a loss and an asymmetric variation of charge density, it was essential to examine the evolution of the internal distribution of the bunch.

The equation of motion of individual particles obeys a second order difference equation. This turn by turn difference equation of the code includes the synchrotron radiation emission through losses, radiation damping, and quantum fluctuations. The long memory of the high Q cavity is retained by the use of propagators. Propagators enable the accurate retention of the phase information of the rapidly oscillating wake over the comparatively long time scale of one revolution period. To get more than an entire relaxation cycle, 10^5 turns were commonly computed for a pop-

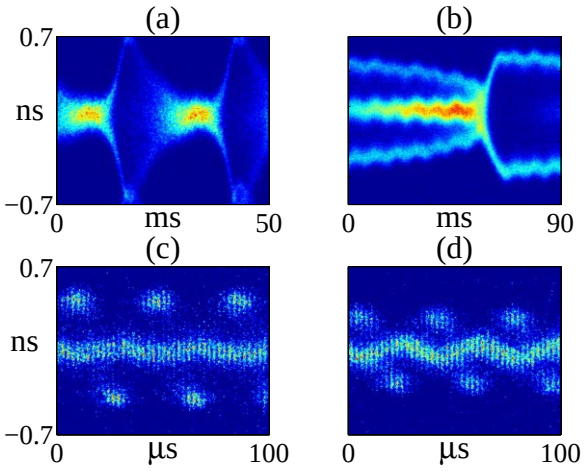

Figure 3: Relaxation cycles for two different values of f_{HOM}: (a) $f_z \sim f_s$. (b) $f_z > f_s$, showing appearance of second center. Note that (b) has much slower damping than (a). (c) Individual streaks are now visible. The second center has more charge than the original main body, yet its oscillation amplitude is still small. (d) The second center now has most of the charge. Its amplitude continues to grow while that of the original main body continues to damp. Oscillations are about π out of phase.

ulation of 20000 particles, distributed over a binning of 300 cells covering the 2π size of the RF bucket.

The wake from the earlier particles is computed by propagating the fields from the previous bin over the time Δt. With $\Phi_t = \omega'_R \Delta t$, the propagator can be represented

$$\begin{pmatrix} W_{t+\Delta t} \\ W'_{t+\Delta t} \end{pmatrix} = e^{-\alpha \Delta t} \begin{pmatrix} \cos\Phi_t & \frac{1}{\omega'_R}\sin\Phi_t \\ -\omega'_R \sin\Phi_t & \cos\Phi_t \end{pmatrix} \times \begin{pmatrix} W_t \\ W'_t \end{pmatrix} + \begin{pmatrix} 2\alpha R_s n_{t+\Delta t} \\ -4\alpha^2 R_s n_{t+\Delta t} \end{pmatrix}$$

3.2 Simulation results

The code is in good agreement with the data. It reproduces the very low frequency of the relaxation oscillation (always below 100 Hz in our case). It confirms qualitatively the evolution of frequency and amplitude as a function of the induced voltage. The code reproduces the $\pi/2$ limit cycle amplitude observed with the streak camera. Finally, the code corroborates the streak camera data, discussed above, that shows the bunch grow as a macroparticle which loses charge density to an attractor at the center (figure 4).

Based on these agreements, the predictions of the code can be viewed with confidence. They were used to gain further insight into the details of the oscillation too sensitive to be seen with our experimental setup. The tracking code phase space distribution shows that the filamentation starts from the head of the bunch. Particles spiral from the head of the bunch towards the center of phase space (figure (4b)). One can observe that those particles perform synchrotron oscillations at a higher frequency than those still attached to the main body. These results gave important clues for the theoretical model.

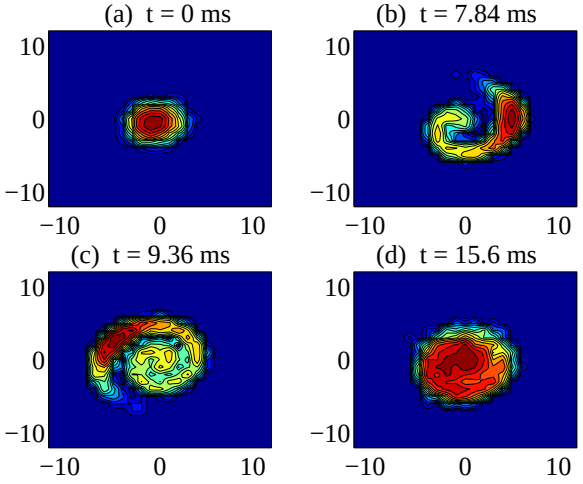

Figure 4: Simulations of bunch in four stages of relaxation oscillation. Intensity scale is logarithmic.

4 CONCLUSION

An extensive campaign of measurements was performed on SPEAR to characterize the low frequency relaxation oscillations produced by long range wakefields. The main features of the relaxation oscillation were: growth of the amplitude of oscillation of the bunch, saturation of the oscillation amplitude, breakup of the bunch, and subsequent damping of the system back to the beginning of the next cycle. The period of this relaxation oscillation is always longer than a radiation damping time. An analytical model was developed to explain these characteristics [3].

5 ACKNOWLEDGEMENTS

We thank H. Wiedemann and M. Cornacchia for their support and encouragement, and we would like to thank our colleagues J. Hinkson and J. Byrd (LBNL), A. Fischer (SLAC) and A. Lumpkin (APS) for their assistance in obtaining the beautiful pictures with the streak camera.

6 REFERENCES

[1] A. Wrulich *et al.*, "Observation of multibunch instabilities in ELETTRA," in *Proc. of EPAC96*, 1996.

[2] G. Rakowsky, "Coherent synchrotron relaxation oscillation in an electron storage ring," in *Proc. of PAC85*, 1985.

[3] J. Sebek and C. Limborg, "Theoretical model of longitudinal relaxation oscillations induced by HOMs," in *Proc. of PAC99*.

[4] J. Sebek and C. Limborg, "Characterization of RF cavity HOMs with beam," in *Proc. of 1997 ICFA Conference*, (Frascati), 1997.